UNIVERSITÀ DEGLI STUDI DI TORINO

Enhancing the efficiency of a dye sensitized solar cell due to the energy transfer between CdSe quantum dots and a designed squaraine dye†

Lioz Etgar,*[a] Jinhyung Park,[b] Claudia Barolo,*[b] Vladimir Lesnyak,*[c] Subhendu K. Panda,[c] Pierluigi Quagliotto,[b] Stephen G. Hickey,[c] Md. K. Nazeeruddin,[a] Alexander Eychmüller,[c] Guido Viscardi[b] and Michael Grätzel[a]

The power conversion efficiency of a dye-sensitized solar cell with tailored squaraine dye enhanced by 47%, due to Förster resonance energy transfer from CdSe quantum dots to the squaraine dye. The incident photons to collection efficiency of electrons indicate panchromatic response from the visible to the near-infrared spectrum.

Introduction

Photovoltaic technology is one of the most promising alternative renewable energy sources, harvesting energy from the sun. Dye sensitized solar cells (DSSCs) are inexpensive and use abundant materials for large-scale solar energy conversion. In a typical DSSC the dye absorbs photons and goes to the excited state, generating electron and hole pairs. The electrons are injected into the TiO_2 conduction band and diffuse to the front contact, simultaneously, the holes are scavenged by a redox couple. Currently DSSCs are exceeding power conversion of 12%,[1] despite the fact that many dyes do not absorb strongly over 700 nm. Therefore, Förster resonance energy transfer (FRET) has already been demonstrated in a variety of optoelectronic applications and recently in DSSCs to harvest visible and near infrared (IR) absorption spectra.[2–5] Usually, the traditional dyes used in DSSCs suffer from low molar extinction coefficients or limited absorption spectra regions.[6] Using FRET to transfer energy from donor to acceptor inside the DSSCs paves a new way for enhancing the photovoltaic performance of DSSCs. This provides the possibility to employ a cascade combination of dyes, which have narrow absorption spectra.

Squaraine dyes are well-known for their remarkable optical behavior because of strong absorption from charge transfer between an electron-deficient central squaric core and each side of the substituent in the red to near-infrared region,[7] and they have been widely and successfully used also in DSSCs in recent years.[8] A recent report on FRET based dye sensitized solar cells showed that the acceptor should be anchored to the TiO_2. In addition it must have lower excitation energy than the donor, enabling fast and efficient electron transfer to TiO_2[9] upon excitation of the energy relay dye.

Quantum dots (QDs) have high molar extinction coefficients and broad absorption spectra covering a wide part of the visible spectrum. Hence they can be good candidates as donors in FRET DSSCs in cases where IR dyes that absorb weakly in the visible region are used as acceptors.

On the other hand, QDs can be affected by the electrolyte, one possibility to avoid this was described by Zaban *et al.*,[10–12] who created an amorphous thin TiO_2 barrier to avoid direct contact with the electrolyte. Another option is to use a more "friendly" electrolyte, which will not quench the QDs.

Here, we apply the FRET concept to a hybrid QDs/dye-sensitized solar cell. The donors are TOP/TOPO-capped CdSe QDs, while the acceptor is a newly designed symmetric squaraine dye, called VG1-C10, possessing an additional carboxylic group[13] as compared to standard squaraine dyes, and two C_{10}-chains. This provides better dye stability and allows efficient energy transfer. The use of the cobalt complex (Co^{+2}/Co^{+3}) as an electrolyte in the cells permits direct contact between the QDs and the electrolyte. Moreover, there is no need to exchange the original ligands of the QDs prior to deposition, since the two C_{10} chains of the dye molecules and TOP/TOPO-capping of the QDs provide the optimum distance for FRET and make the preparation and the structure of the cell simple. As a result of the energy transfer, the cell power conversion efficiency was increased and its solar response was expanded from the visible to the near infrared spectral region.

Results and discussion

Different non-symmetric and symmetric squaraines were synthesized and characterized (see ESI†) in order to match their optical and hydrophobic properties with the selected QDs. Their interaction properties have been studied both in solution and on FTO glass, avoiding the titania substrate in order to eliminate the injection problem. Subsequently, the best couple (symmetrical long chain dyes VG1-C10 and CdSe TOP/TOPO capped QDs) have been used in the cell.

[a]*Laboratoire de Photonique et Interfaces, Institut des Sciences et Ingénierie Chimiques, Ecole Polytechnique Fédérale de Lausanne (EPFL), Station 6, CH-1015, Lausanne, Switzerland. E-mail: lioz.etgar@epfl.ch*
[b]*Dipartimento di Chimica, NIS Centre of Excellence, Università di Torino, Via Pietro Giuria 7, I-10125, Torino, Italy. E-mail: claudia.barolo@unito.it*
[c]*Physical Chemistry, TU Dresden, Bergstr. 66b, 01062, Dresden,*

The symmetric squaraine VG1-C10 was synthesized *via* a two step procedure using commercially available precursors (see Scheme 1). Symmetrical dyes have the advantage of simple synthesis and easy purification by crystallization.[13] For the synthesis details and NMR data see the ESI.†

The scheme of the energy transfer cell is presented in Fig. 1A. The TiO_2 electrode was first dipped in the VG1-C10 dye solution overnight and then the CdSe QDs were spin coated on top of the dye-coated electrode. Finally the Co^{+2}/Co^{+3} electrolyte was injected into the cell.

Fig. 1B shows the energy level diagram of the cell, which is a type I system. The energy level positions of the QDs and of the dye permit energy transfer between the QDs as donor and the dye as the acceptor. Moreover, the mismatch in the conduction band of the QDs and the LUMO of the dye does not allow for charge transfer from the dye to the QDs. As a rule, in the DSSC light is absorbed by the dye, an electron is excited from the HOMO to the LUMO and injected to the conduction band of TiO_2. In the present hybrid cell, the QDs act as additional light harvesters absorbing the light and transferring the energy of their excited state to the LUMO of the dye *via* dipole–dipole interaction. Subsequently, as in standard DSSCs, the electron from the LUMO of the dye is injected to the conduction band of the TiO_2 and the hole is transported to the counter electrode *via* the redox couple.

Fig. 2 shows FTIR spectra of the VG1-C10 as dye powder in KBr pellets and the VG1-C10 adsorbed on TiO_2. The spectra reveal that the adsorption of VG1-C10 on TiO_2 occurs *via* carboxy groups, showing two bands at 1609 cm^{-1} and 1353 cm^{-1},[14] while the characteristic COOH band around 1730 cm^{-1}–1680 cm^{-1} completely disappeared. Therefore, the VG1-C10 can be linked by both COOH groups to the titania surface, in a *cis* arrangement, probably directing the hydrocarbon chains far from the TiO_2.

Relying on the FTIR measurements, Fig. 1C presents a possible explanation for the orientation of the QDs and the dye inside the cell, which permits FRET to occur. As discussed above, the VG1-C10 dye anchors the TiO_2 by using its two carboxylic groups, as a result the $C_{10}H_{21}$-chains are free and away from the TiO_2, which allows them to intertwine with the TOP/TOPO ligands of the QDs *via* efficient hydrophobic interactions. This kind of a connection results in an average distance between the donor and the acceptor, which lies within the Förster radius and allows an efficient energy transfer. This type of ligand interconnection was demonstrated by Vogel *et al.*[15] showing FRET between QDs and lipids both containing long hydrocarbon chains.

Fig. 3 shows the absorption and emission spectra of the CdSe QDs and the VG1-C10 dye. For FRET it is essential that the emission spectrum of the donor (QDs) overlap with the absorption spectrum of the acceptor (dye).

The Förster radius, R_0, is the distance at which the probability for energy transfer is 50%. The Förster radius is given by:[16]

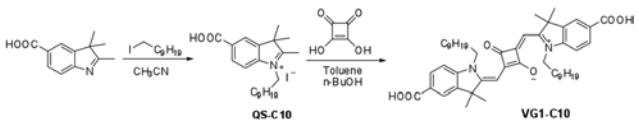

Scheme 1 Synthetic pathway for symmetric squaraine VG1-C10.

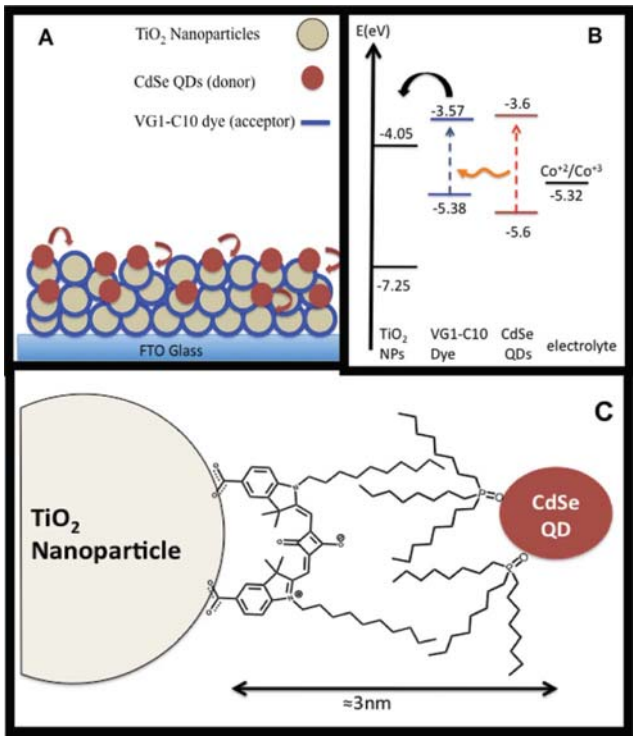

Fig. 1 (A) Schematic presentation of the cell structure; (B) energy level diagram of the components involved in the cell. Dashed arrows represent absorption, wavy arrows show energy transfer from the QDs excited state to the LUMO of the dye *via* dipole–dipole interaction; (C) the arrangement of the QDs and the VG1-C10 inside the cell.

$$R_0^6 = \frac{9000(\ln 10)\kappa^2 Q_D J}{128\pi^5 n^4 N_{AV}} \quad (1)$$

where n is the refractive index of the medium (typically 1.4–1.5 for the electrolytes employed in DSSCs), κ^2 is the orientation factor (2/3 for random orientation), Q_D is the quantum yield (QY) of the donor (28%), N_{av} is the Avogadro number, J is the overlap integral:

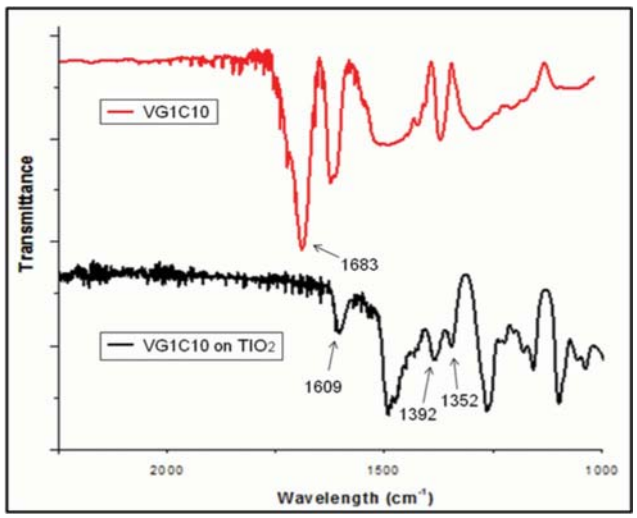

Fig. 2 FTIR spectra of VG1-C10 in KBr pellets (red), and VG1-C10 adsorbed on TiO_2 electrodes (black).

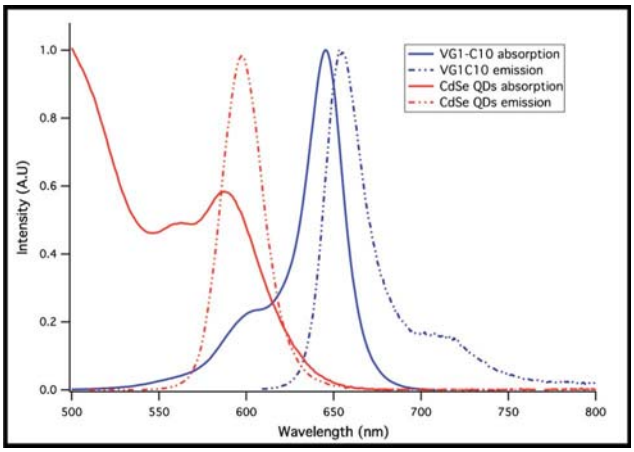

Fig. 3 Absorption and emission spectra of the CdSe QDs and VG1-C10 dye.

$J = \int_0^\infty I_D(\lambda)\varepsilon_A(\lambda)\lambda^4 d\lambda$, I_D is the emission profile spectrum of the donor and ε_A is the molar extinction coefficient of the acceptor. According to this formula, R_0 in our system is 3.7 nm, which agrees well with our suggested orientation of the QDs and the dye. One of the main evidences for FRET is the shortening of the donor lifetime in the presence of the acceptor and the increase of the lifetime of the acceptor in the presence of the donor.

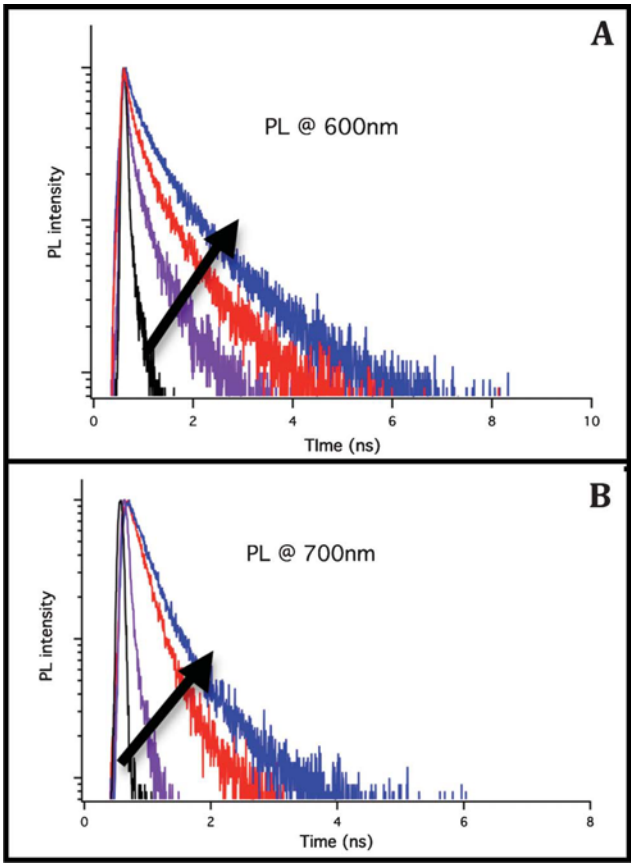

Fig. 4 Time resolved PL spectra of the composite QDs/VG1C10 films with different ratios recorded at 600 nm (QDs emission) (A) and at 700 nm (VG1-C10 emission) (B); λ_{ex} = 470 nm for all the samples except the pure VG1-C10 film excited at 635 nm (black curve in Fig. 4B). Note, QDs emission measured at 700 nm (ex. 470 nm) is very weak (not shown). The arrows indicate an increase in the QD/VG1 ratio.

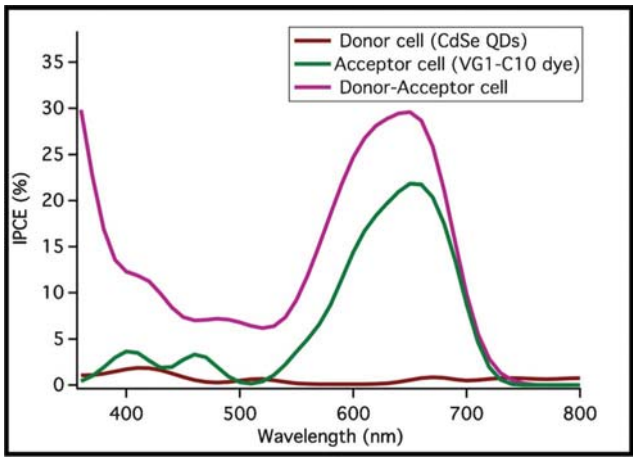

Fig. 5 Incident photon to current efficiency (IPCE) curves of the three cells. The CdSe cell (brown line); the VG1-C10 cell (green line) and the hybrid cell composed of the donor and acceptor (purple line).

In order to show the energy transfer from the CdSe QDs to the VG1-C10 dye, mixed composite films of different QDs/VG1-C10 ratios were prepared. Absorption and photoluminescence (PL) spectra of the CdSe QDs and the VG1-C10 dye in solution are presented in Fig. 3. As is seen from the figure, the QDs sample chosen for the experiments as a potential energy donor meets two main requirements for investigation of energy relations in the system by means of optical spectroscopy: on the one hand, its emission spectrum overlaps with the absorption of the dye, on the other hand its PL maximum is quite distant from that of the dye, which allows for the separate detection of the time resolved emissions from the donor and from the acceptor, at 600 and 700 nm, respectively. Moreover, excitation sources for time resolved measurements (pulse laser diodes) allow for separate excitation of the QDs and the dye. As is seen from Fig. 3, neither the QDs absorb light at 670 nm (used for the dye emission measurements), nor does the dye absorb at 470 nm (used for the QDs PL excitation). Thus, emissions of the QDs and the dye do not interfere and consequently do not account for time resolved traces of each other.

As is clearly seen from Fig. 4A and B, an increase in the QDs content in the mixed films leads to strong enhancement of both

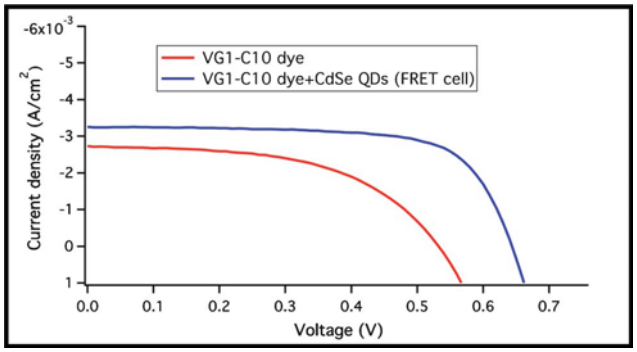

Fig. 6 Photovoltaic response of the VG1-C10 cell and the VG1-C10 + CdSe QDs cell.

Table 1 Photovoltaic performance of the VG1-C10 dye (acceptor) cell and of the donor/acceptor cell, showing the improvement of the performance due to the FRET

Cell type	J_{sc}/mA cm^{-2}	V_{oc}/mV	FF	η @ 1 sun
VG1-C10 dye	2.73	542	0.536	0.79
VG1-C10 dye + CdSe QDs (FRET cell)	3.25	653.4	0.69	1.48
Δ	+16%	+17%	+23%	+47%

emission lifetimes. Thus the more donors present in the system, the more efficient energy pumping of the acceptor is realized. FRET from the donors (QDs) is clearly shown by the appearance of a slow component in the acceptor PL lifetime.

FRET efficiency can be calculated according to the following equation:[17] $E = 1 - (\tau_{DA}/\tau_D)$, where τ_{DA} and τ_D are the lifetime of the donor in the presence of the acceptor and the lifetime of the donor alone, respectively. In our case, the PL lifetime was fitted by bi-exponential equation and the weighted average lifetime of each decay curve was calculated. The donor lifetime is 9.7 $\pm$ 0.1 ns and the lifetime of the donor in the presence of acceptor drops to 3 $\pm$ 0.1 ns. For the lifetime of the donor in the presence of the acceptor, we considered the QD/VG1-C10 ratio, which is the same as their ratio in the cell. The calculated FRET efficiency is E $\approx$ 69%.

Fig. 5 shows the incident photon to current efficiency (IPCE) of three different DSSCs: CdSe QDs donor cell, VG1-C10 acceptor cell and hybrid cell composed of the donor (QDs) and the acceptor (dye). The QDs cell (one layer of QDs deposited on the titania electrode) shows a very week response for the whole wavelength range. The dye cell exhibits an IPCE response between 500 nm to 750 nm, which matches well the absorption spectrum of the dye (see Fig. 3). As is seen from Fig. 5, the hybrid cell containing both the dye and the QDs layers has the best efficiency and demonstrates response over the whole visible range, reaching its maximum at 360 nm and 660 nm, corresponding to IPCE intensity of 36% and 30%, respectively. The coverage of the whole visible spectrum in the hybrid cell is evidence for the efficient FRET interaction between the constituents of the light-absorbing layer. Moreover, the cell fabrication method, consisting of dipping the TiO_2 electrode in the dye solution with subsequent deposition of the QDs *via* spin coating, minimizes the possibility of co-sensitization. During the QDs deposition the whole TiO_2 surface is already covered by the dye molecules, which prevents direct injection of electrons from the QDs to the TiO_2 conduction band.

The photovoltaic performance (PV) of the acceptor cell composed of the VG1-C10 dye only and the donor-acceptor cell (composed of the dye and the QDs) is shown in Fig. 6 and Table 1. The acceptor cell exhibits a power conversion efficiency (PCE) of 0.79% under AM 1.5 G and short circuit current (J_{sc}), open circuit voltage (V_{oc}), and fill factor (FF) of 2.73 mA cm^{-2}, 542 mV, and 0.53, respectively. Upon incorporation of CdSe QDs into the device, the J_{sc} increases by 16% to 3.25 mA cm^{-2} with an increase in the PCE up to 1.48%. The V_{oc} increased by 111 mV (17% increase) and the FF increased by 23%. The increase in the V_{oc} is mainly due to an upward shift of the TiO_2 conduction band. This can be explained in the difference of the dark current measurements shown in Fig. 7 (assuming the same recombination behaviour), and by the higher current density of the FRET cell, which indicates more electrons injected into the TiO_2 conduction band. The 47% increase in the device efficiency is partially attributed to the increase in the J_{sc} due to the harvesting of visible photons in the 350–650 nm region resulting from energy transfer.

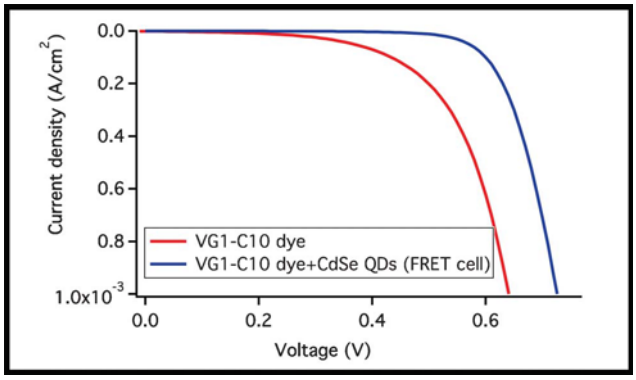

Fig. 7 Dark current measurements of the VG1-C10 cell and the VG1-C10 + CdSe QDs cell (FRET cell).

Conclusion

We demonstrated an enhancement of the light harvesting in dye sensitized solar cell due to Förster resonance energy transfer. The donors are CdSe QDs and the acceptor is a new designed symmetric squaraine dye with two carboxy groups and two long hydrocarbon chains. The use of the cobalt complex (Co^{+2}/Co^{+3}) as the electrolyte in the cells permits direct contact between the QDs and the electrolyte without affecting the QDs, which results in a simple structure FRET system employed in a hybrid QDs/dye-sensitized solar cell. PL lifetime measurements revealed FRET from the QDs to the dye. IPCE curves of the device exhibit a full coverage of the visible region. In addition, all the cell photovoltaic parameters were enhanced, proving efficient energy transfer within the QD–dye-sensitized solar cell.

Acknowledgements

This research was funded by the European Community's Seventh Framework Programme (FP7/2007-2013) under grant agreement n° 227057, Project "INNOVASOL". L. E. acknowledges the Marie Curie Actions-Intra-European Fellowships (FP7-PEOPLE-2009-IEF) under grant agreement n° 252228, project "Excitonic Solar Cell". We gratefully acknowledge Christian Waurisch (TU Dresden) for providing the samples. J. P., C. B., P. Q. and V. G. thank Compagnia di San Paolo and Fondazione CRT for continuous equipment supply.

References

1 A. Yella, H.-W. Lee, H. N. Tsao, C. Yi, A. K. Chandiran, Md. K. Nazeeruddin, E. W.-G. Diau, C.-Y. Yeh, S. M. Zakeeruddin and M. Grätzel, *Science*, 2011, **334**, 629.

2 B. E. Hardin, E. T. Hoke, P. B. Armstrong, J. H. Yum, P. Comte, T. Torres, J. M. J. Frechet, M. K. Nazeeruddin, M. Grätzel and M. D. McGehee, *Nat. Photonics*, 2009, **3**, 406.

3 K. Shankar, X. Feng and C. A. Grimes, *ACS Nano*, 2009, **3**, 788.

4 J. H. Yum, B. E. Hardin, S. J. Moon, E. Baranoff, F. Nüesch, M. D. McGehee, M. Grätzel and M. K. Nazeeruddin, *Angew. Chem., Ger. Edit.*, 2009, **48**, 9277.

5 K. Driscoll, J. Fang, N. Humphry-Baker, T. Torres, W. T. S. Huck, H. J. Snaith and R. H. Friend, *Nano Lett.*, 2010, **10**, 4981.

6 A. Hagfeldt, G. Boschloo, L. Sun, L. Kloo and A. H. Pettersson, *Chem. Rev.*, 2010, **110**, 6595.

7 (*a*) S. Yagi, Y. Hyodo, M. Hirose, H. Nakazumi, Y. Sakurai and A. Ajayaghosh, *Org. Lett.*, 2007, **9**, 1999; (*b*) W. Y. Yan, A. L. Sloat, S. Yagi, H. Nakazumi and C. L. Colyer, *Electrophoresis*, 2006, **27**, 1347; (*c*) M. Matsui, S. Tanaka, K. Funabiki and T. Kitaguchi, *Bull. Chem. Soc. Jpn.*, 2006, **79**, 170; (*d*) N. Fu, J. M. Baumes, E. Arunkumar, B.C. Noll and B.D. Smith, *J. Org. Chem.*, 2009, **74**, 6462.

8 (*a*) J.-H. Yum, P. Walter, S. Huber, D. Rentsch, T. Geiger, F. Nesch, F. De Angelis, M. Grätzel and M. K. Nazeeruddin, *J. Am. Chem. Soc.*, 2007, **129**, 10320; (*b*) T. Geiger, S. Kuster, J.-H. Yum, S.-J. Moon, Md. K. Nazeeruddin, M. Grätzel and F. Nüesch, *Adv. Funct. Mater.*, 2009, **19**, 2720; (*c*) S. Paek, H. Choi, C. Kim, N. Cho, S. So, K. Song, M. K. Nazeeruddin and J. Ko, *Chem. Commun.*, 2011, **47**, 2874–2876; (*d*) Y. Shi, R. B. M. Hill, J.-H. Yum, A. Dualeh, S. Barlow, M. Grätzel, S. R. Marder and M. K. Nazeeruddin, *Angew. Chem., Int. Ed.*, 2011, **50**, 6619–6621.

9 (*a*) K. Shankar, X. Feng and C.A. Grimes, *ACS Nano*, 2009, **3**, 788; (*b*) J. I. Basham, G. K. Mor and C. A. Grimes, *ACS Nano*, 2010, **4**, 1253; (*c*) G. K. Mor, J. Basham, M. Paulose, S. Kim, O. K. Varghese, A. Vaish, S. Yoriya and C. A. Grimes, *Nano Lett.*, 2010, **10**, 2387.

10 S. Buhbut, S. Itzhakov, E. Tauber, M. Shalom, I. Hod, T. Geiger, Y. Garini, D. Oron and A. Zaban, *ACS Nano*, 2010, **4**, 1293–1298.

11 S. Buhbut, S. Itzhakov, D. Oron and A. Zaban, *J. Phys. Chem. Lett.*, 2011, **2**, 1917.

12 S. Itzhakov, S. Buhbut, E. Tauber, T. Geiger, A. Zaban and D. Oron, *Adv. Energy Mater.*, 2011, **1**, 626.

13 J. Park, C. Barolo, F. Sauvage, N. Barbero, C. Benzi, P. Quagliotto, S. Coluccia, D. Di Censo, M. Grätzel, M. K. Nazeeruddin and G. Viscardi, *Chem. Commun.*, 2012, **48**, 2782–2784.

14 (*a*) K. Y. Law, F. C. Bailey and L. J. Bluett, *Can. J. Chem.*, 1986, **64**, 1607; (*b*) E. Terpetschnig, H. Szmacinski, A. Ozinskas and J. R. Lakowicz, *Anal. Biochem.*, 1994, **217**, 197.

15 I. Geissbuehler, R. Hovius, K. L. Martinez, M. Adrian, K. R. Thampi and H. Vogel, *Angew. Chem., Int. Ed.*, 2005, **44**, 1388–1392.

16 T. Förster, Transfer Mechanisms of Electronic Excitation. Discuss., *Faraday Soc.*, 1959, 7.

17 J. R. Lakowicz, *Principles of Fluorescence Spectroscopy*, Plenum Press, New York and London, 3rd edn, 1986, pp. 496.

SUPPORTING INFORMATION

Enhancing the efficiency of a dye sensitized solar cell due to the energy transfer between CdSe quantum dots and a designed Squaraine dye

Etgar Lioz[a]*, Park Jinhyung[b], Barolo Claudia[b]*, Lesnyak Vladimir[c] *, Panda Subhendu K.[c], Quagliotto Pierluigi[b], Hickey Stephen G.[c], Md. K. Nazeeruddin[a], Eychmüller Alexander[c], Viscardi Guido[b], Grätzel Michael[a]

[a] Laboratoire de Photonique et Interfaces, Institut des Sciences et Ingénierie Chimiques, Ecole Polytechnique Fédérale de Lausanne (EPFL), Station 6, CH-1015, Lausanne, Switzerland.

[b] Dipartimento di Chimica Generale e Chimica Organica, NIS Centre of Excellence, Università di Torino, Corso Massimo D'Azeglio 48, I-10125, Torino, Italy.

[c]Physical Chemistry, TU Dresden, Bergstr. 66b, 01062 Dresden, Germany.

*lioz.etgar@epfl.ch, claudia.barolo@unito.it, vladimir.lesnyak@chemie.tu-dresden.de

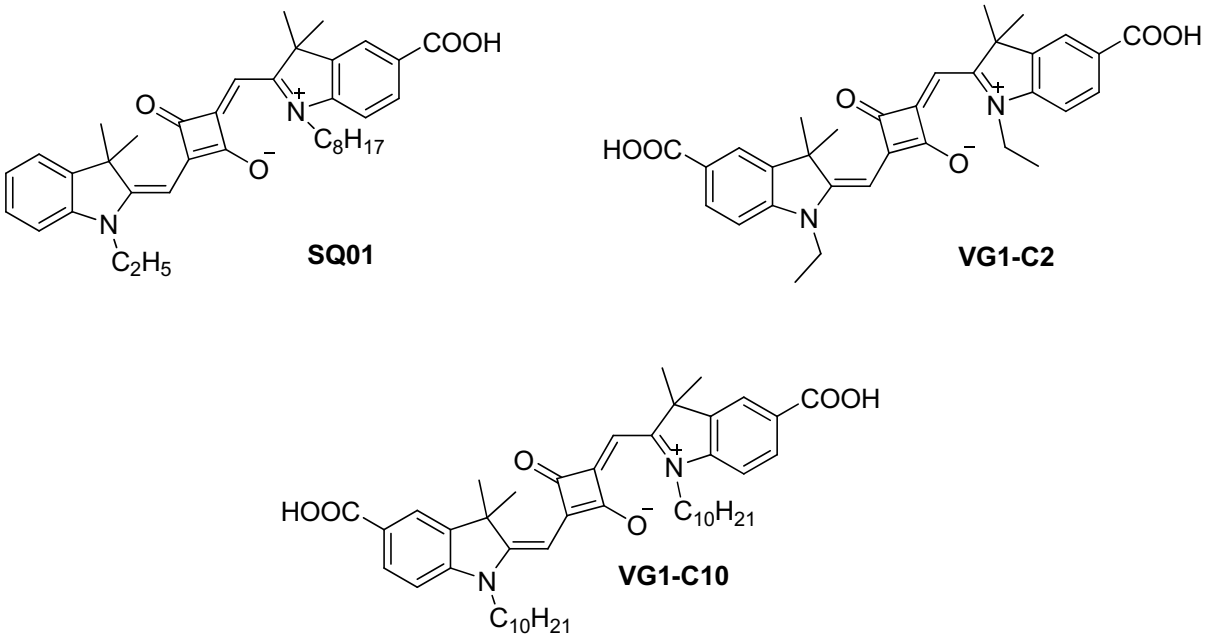

Figure 1-SI Structures of the studied squaraines.

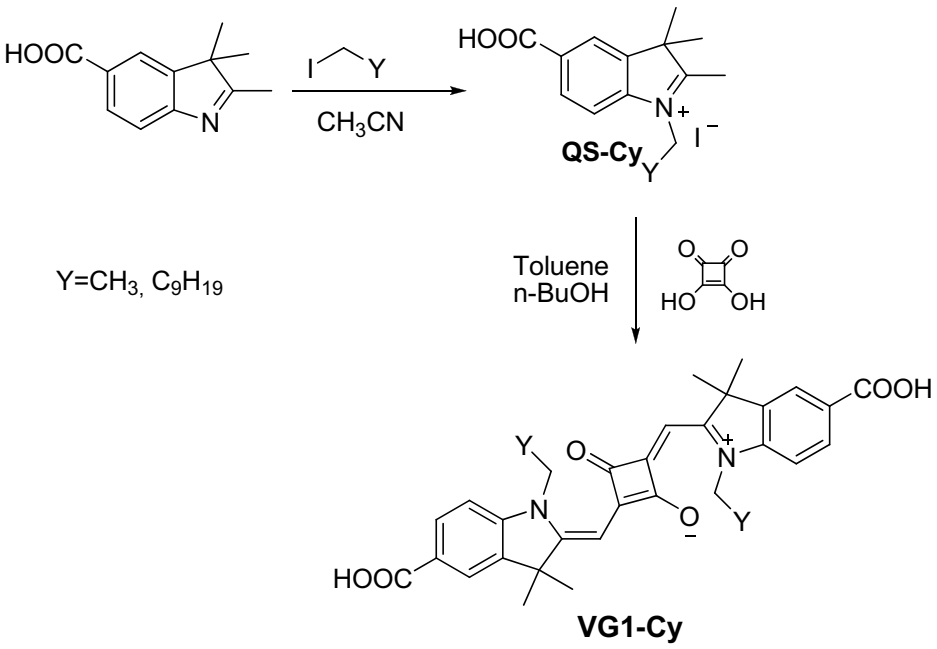

Scheme 1 SI: Synthetic pathway

1. Synthesis

1.1 CdSe QDs synthesis

All reactions were performed under an inert Ar atmosphere on a Schlenk line. Cadmium oxide (CdO, 99%), 1-hexadecylamine (HDA, 99%), tri-n-octylphosphine (TOP, 90%), and tri-n-octylphosphineoxide (TOPO, 99%) were purchased from Aldrich. Selenium powder (Se, 99.99%) was purchased from Chempur. Prior to their use HDA was degassed at 100 °C for 30 min while TOPO and TOP were degassed at 190 °C for 1 h.

In a three-neck flask, 0.2 mmol of CdO and 0.5 g of stearic acid were heated to 180 °C until the mixture became clear and then cooled down to room temperature. 3 ml of HDA and 6 ml of TOPO were added to the mixture and degassed again at 100 °C for 15 minutes. The mixture was then heated to 310 °C under vigorous stirring and 1 ml of 1 M TOPSe was swiftly injected. The temperature was lowered to 280 °C for the nanocrystal growth for ~3 minutes. The heating was removed after the desired sized particles (emission at 600 nm) were formed and then the solution was suddenly cooled to room temperature by putting a water bath. To isolate the QDs, a toluene/methanol (MeOH) (1:1 vol:vol) mixture was added, followed by centrifugation at 3000 rpm for 5 minutes. The resulting precipitate could readily be dispersed in a number of organic solvents, including hexanes, toluene or chloroform.

1.2 Synthesis of squaraine dyes

1.2.1 Materials and structural characterization

All the chemicals were purchased from Sigma Aldrich, and were used as received. The glassware used for the quaternarization synthesis was heated overnight in an oven at 150°C and assembled in the oven, then cooled under Ar flux before starting the reactions. TLC was performed on silica gel 60 F254 plates using dichloromethane (DCM) and MeOH (90:10) as eluents.

ESI-MS spectra (positive ions) were recorded using a LCQ Deca XP plus spectrometer (Thermo), with electrospray interface and ion trap as mass analyzer. The flow injection effluent was delivered into the ion source using nitrogen as sheath and auxiliary gas.

^{1}H NMR (200 MHz) and ^{13}C NMR (50 MHz) spectra were recorded on a Bruker Avance 200 NMR in acetone, dimethylsulfoxide-d_6 (DMSO-d_6) using their signals as a reference. NMR signals are described by use of s for singlet, d for doublet, t for triplet, m for multiplet.

SQ01, QS-C2, VG1-C2 were synthesized and characterized previously[1].

1.2.2 QS-C10

1.5 g (7.38 mmol) of 2,3,3-trimethyl-3*H*-indole-5-carboxylic acid and 5.9 g of 1-iododecane were dissolved in 50 ml CH_3CN and refluxed under argon for 24 h. The solvent was evaporated and the crude product was washed with diethyl ether several times and filtered off. The product obtained was a pink powder. 1.8 g (51.7 %); ^{1}H NMR (200 MHz, DMSO-d_6): ppm = 8.37 (s, 1H), 8.30 (d, J = 8.0 Hz 1H), 7.99 (d, J = 8.0 Hz, 1H), 4.54 (t, 2H), 1.97 (m, 2H), 1.56-1.40 (m, 14H), 1.65 (s, 3H), 1.29 (s, 6H), 0.88 (t, 3H).

1.2.3 VG1-C10

1 g (2.12 mmol) of 5-carboxy-2,3,3-trimethyl-1-decyl-3*H*-indolium iodide and 120 mg of 3,4-dihydroxycyclobut-3-ene-1,2-dione were dissolved in a mixture of 10 ml toluene and 10 ml *n*-butanol. The mixture was refluxed with a Dean-Stark apparatus for 6 h. After 10 min the solution turned green and after 1 h to blue-green color. The solvent was removed by distillation until the product precipitated. The crude product was recrystallized with n-butanol and filtered off. The

[1] a) J. Park, C. Barolo, F. Sauvage, N. Barbero, C. Benzi, P. Quagliotto, S. Coluccia, D. Di Censo, M. Grätzel, M. K. Nazeeruddin, G. Viscardi, *Chem. Commun.* **2012**, accepted; b) S. Kuster, F. Sauvage, M. K. Nazeeruddin, M. Grätzel, F. A. Nüesch and T. Geiger, *Dyes and Pigments*, 2010, **87**, 30-38

product was obtained as a blue-grey powder. 437 mg (53.9%) ^{1}H NMR (200 MHz, DMSO-d_6) ppm = 8.03 (s, 2H), 7.97 (d, 2H), 7.44 (d, 2H), 5.90 (s, 2H), 4.13 (q, 4H), 1.70 (s, 12H), 1.40–1.20 (m, 32H), 0.86 (t, 6H). ^{13}C NMR (50MHz, Acetone-d_6) ppm = 182.06, 180.59, 169.90, 167.09, 146.13, 141.71, 130.28, 126.26, 123.20, 109.88, 87.78, 48.68, 31.79, 26.68, 26.37, 22.22, 13.53. MS (ESI-) *m/z*: 763.50 [764.48 calcd. for [($C_{48}H_{64}N_2O_6$)]

2. Experimental procedures

2.1 UV spectra - Determination of the λ_{max} and molar absorption coefficients

A certain amount of the dye (typically 7-10 mg) was dissolved in 10 ml of DMSO. 0.25 ml aliquot of this solution was diluted to 25 ml with a proper solvent (stock solution). Three samples were performed by diluting 1.0, 2.5 and 5 ml of this solution to 25 ml. The solutions obtained were analyzed by UV-Vis spectroscopy (Cary 300 Bio) using quartz cuvettes (1 cm pathway length). Absorbance at the λ_{max} for the each solution was plotted vs. dye concentration with subsequent linear fitting. The slope of the plot is the molar absorption coefficient (ε). For the purpose of reproducibility this determination was repeated twice by preparing two more dye stock solutions in DMSO which were subjected to the same dilution procedure. The logε obtained from the two separate data sets were compared: if their difference was less or equal to 0.02 with respect to their average values, the data were considered acceptable and the average of the two values was taken. Otherwise, one more dye stock solution was prepared; the whole procedure was repeated until the difference of 0.02 was attained.

2.2 Fluorescence Emission spectra

Fluorescence measurements were performed using a Fluorolog 2 (Jobyn Ivon). The excitation wavelength was set at 600 nm. A few mg of the dye was loaded in a test tube and a few ml of a proper solvent were added. The test tubes were sonicated for approx. 1 min, and left for about 30 minutes to accomplish complete solubilization. The sample was used to prepare more diluted solutions, and their absorbance at λ_{max} was determined in order to ensure that the absorbance is maintained lower of 0.1 units of absorbance. For every solution fluorescence emission spectrum was detected and λ_{em} was obtained.

Two standards, Rhodamine 101 dissolved in EtOH/0.01 M HCl and Cresyl Violet in MeOH, were measured under the same conditions as for squaraine samples.

Operative conditions (Rhodamine 101 quantum yield = 0.96 and Cresyl Violet = 0.54)[2]:

- Rhodamine 101: λ_{ex} = 535, emission range: 545-800 nm, excitation and emission slits: 3 nm.
- Cresyl Violet: λ_{ex} = 520, emission range: 530-800 nm, excitation and emission slits: 3 nm.

The quantum yield[3] is determined by:

$$\phi_x = \phi_{ST} \frac{A_x}{A_{ST}} \frac{I_{ST}}{I_X} \left(\frac{\eta_x^2}{\eta_{ST}^2} \right) \qquad \text{(eq. 1)}$$

where Φ_x is the measured quantum yield for the sample, Φ_{ST} in the quantum yield of the standard dye (Rhodamine 101 or Cresyl violet), A_x and A_{ST} are the integrated areas under the fluorescence emission curve of the sample and the standard reference respectively, I_{ST} and I_x are the absorbance of the standard dye and the sample respectively, η_x and η_{ST} are the refractive indexes for the solvents in which the sample and the standard reference are dissolved respectively. The reported quantum yield is the average of the values obtained vs Rhodamine 101 and Cresyl Violet respectively.

[2] *Anal. Chem.*, **2009**, 81, 6285-6294

[3] Lakowicz JR. Principles of fluorescence spectroscopy. New York: Springer- Verlag; 2006.

Fluorescence lifetimes were obtained on a Fluorolog 2 spectrofluorimeter equipped with a NanoLED source (emitting at 635nm) using a photon counting detector (TBX04). The fluorescence decay was recorded at 650 or 670 nm.
The same solutions as for the quantum yield determination were used. The data were fitted to a single exponential function giving the lifetime.

2.3 IR Spectroscopy measurements
FT-IR spectra of the dye powder were recorded in KBr pellets on a Shimadzu FT-IR Spectrometer (FTIR 8400). The resolution was set at 1 nm and the data were baseline subtracted and treated with triangle apodization function. Dyes adsorbed on TiO_2 electrodes were analyzed using ATR (diamond, MKII Golden Gate) from Specac.

2.4 Optical Characterization of QDs
UV-Vis absorption spectra were recorded using a Cary 50 spectrophotometer (Varian Inc.). Fluorescence measurements were performed with a FluoroMax-4 spectrofluorimeter (HORIBA Jobin Yvon Inc.). Time resolved PL traces were recorded on a Fluorolog-3 spectrofluorimeter (HORIBA Jobin Yvon Inc.) using a 200 ps pulsed laser diodes emitting at 470 nm and 635 nm (for pure VG1-C10 film). All measurements were performed at room temperature. The PL QY of the CdSe QDs was evaluated according to the procedure described in ref.[1] using Rhodamine 6G and Rhodamine 101 solutions in ethanol as reference standards (PL QY = 95 and 96%, respectively).

2.5 CdSe QDs/VG1-C10 composite films preparation
Composite films were prepared by drop-casting QDs+VG1-C10 mixtures of different compositions in THF onto quartz glass plates with subsequent drying.

3. Optical Characterization

3.1 Optical Characterization of squaraine dyes

3.1.1 UV-VIS

UV-VIS spectra were collected for the squaraine dyes using six different solvents: THF, DCM, DMSO, acetonitrile (ACN), ethanol (EtOH) and MeOH, in the concentration range of $1 \cdot 10^{-6}$ - $5 \cdot 10^{-5}$ M. The spectra showed substantial negative solvatochromism: the λ_{max} decreases when the solvent polarity increases. The solvatochromic behaviour is demonstrated in Figure 2-SI and solvatochromic data along with logε, FWHM (Full Width at Half Maximum) and the oscillator strength are reported in Table 1-SI,

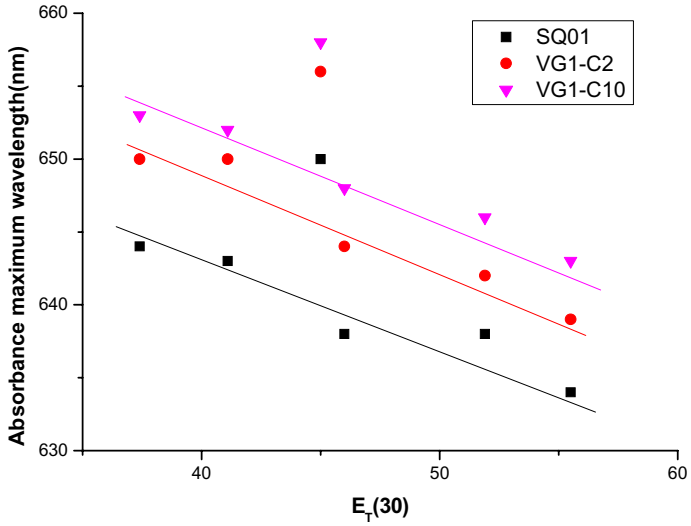

Figure 2-SI: negative solvatochromic behaviour for UV-Vis λ_{max} vs $E_T(30)$, line is from regression, excluding DMSO outlier data .

Table 1-SI: Absorption maxima (λ_{max}) for the SQ01 and VG1-C10 squaraines in different solvents

Solvent	SQ01				VG1-C2				VG1-C10			
	λ_{max}	Logε	FWHM	O. Str.	λ_{max}	Logε	FWHM	O. Str.	λ_{max}	Logε	FWHM	O. Str.
THF	644	5.39	592	0.63	650	5.48	556	0.73	653	5.53	577	0.84
DCM	643	5.38	611	0.63	650	5.60	564	0.97	652	5.57	583	0.94
DMSO	650	5.21	590	0.41	656	5.45	596	0.73	658	5.41	644	0.72
ACN	638	5.30	670	0.58	644	5.44	602	0.72	648	5.48	620	0.81
EtOH	638	5.36	589	0.58	642	5.43	590	0.69	646	5.44	649	0.77
MeOH	634	5.39	632	0.67	639	5.47	583	0.74	643	5.52	621	0.89

A careful analysis of the λ_{max} shift reveals that the addition of the second carboxyl group (asymmetric squaraine SQ01 vs symmetric VG1-C10) leads to a red shift of 6 nm. The oscillator strength, while varying for different solvents, is high for VG1-C10. This accounts for a better ability of symmetric molecules to absorb light than the asymmetric ones confirming the literature data. A study of the aggregation ability of these dyes was performed in EtOH, since it was used for dye absorption onto TiO_2. The correlation with concentration was linear with excellent r^2= 0.999. The aggregation was thus excluded in the concentration range examined.

3.1.2 Fluorescence Measurements

Fluorescence emission was studied in the same solvents used for the UV spectra. The dyes were studied by the steady-state and time resolved spectroscopy.

Spectra acquired in the different solvents gave the solvatochromic results shown in Figure 3-SI and summarized in Table 2-SI. The emission maximum, the Stokes shift and the $E_{0\text{-}0}$ transition were determined.

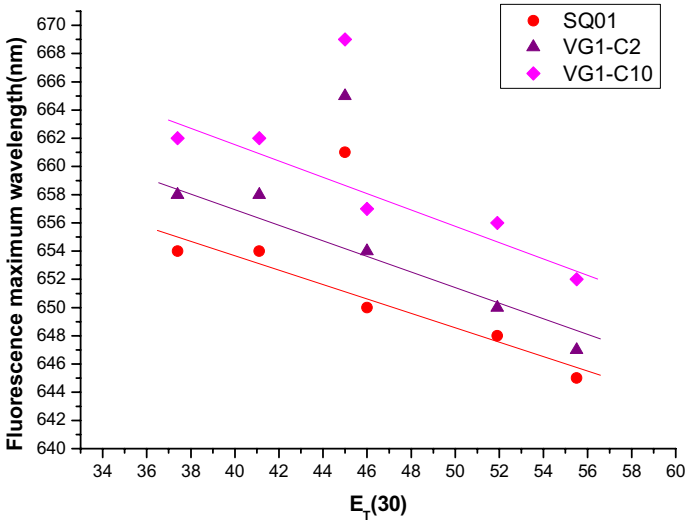

Figure 3-SI: Emission properties of squaraine VG1-C10: line is from regression, excluding DMSO data.

Table 2-SI: Emission maxima (λ_{em}) for the squaraine VG1-C10 in different solvents.

Solv.	SQ01			VG1-C2			VG1-C10		
	λ_{em} [nm]	Stokes Shift	$\Delta E_{0\text{-}0}$ [eV]	λ_{em} [nm]	Stokes Shift	$\Delta E_{0\text{-}0}$ [eV]	λ_{em} [nm]	Stokes Shift	$\Delta E_{0\text{-}0}$ [eV]
THF	648			654	10.0	1.91	662	9	1.89
DCM	650	13.5	1.93	654	11.5	1.91	662	10	1.89
DMSO	656	12.5	1.91	661	11.0	1.89	669	11	1.87
ACN	646	15.0	1.95	650	11.5	1.93	657	9	1.89
EtOH	642	12.0	1.95	648	9.5	1.93	656	8	1.91
MeOH	642	13.5	1.96	645	10.5	1.94	652	9	1.91

The negative solvatochromic behavior, already shown for the UV spectra, was evident also in the emission spectra. DMSO behaves anomalously also in this case. From the intersection of the absorption and emission spectra the zeroth-zeroth transition $\Delta E_{0\text{-}0}$ was evaluated. $\Delta E_{0\text{-}0}$ correlates with solvent polarity in agreement with the solvent polarity dependence for λ_{max}. The transition gap increases (while λ_{max} decreases) with solvent polarity. In agreement with the UV-VIS results, the incorporation of a second carboxyl leads to the red shift of λ_{em} of about 6 nm. An analysis of the Stokes shifts shows that for the symmetrical squaraine VG1-C10 the Stokes shift is in the range of 8-16 nm. The introduction of two carboxyl groups slightly reduces the $E_{0\text{-}0}$ value and this is in agreement with a larger extension of the conjugation which is also reflected by the λ_{max} red shift.

The quantum yields and the results of time resolved spectroscopy are shown in Table 3-SI.

Table 3-SI: Lifetime, quantum yield, fluorescence constant and non-radiative constant for the squaraines

	SQ01				VG1-C10			
Solvent	τ	ϕ_{fl}	k_{fl}	k_{nr}	τ	ϕ_{fl}	k_{fl}	k_{nr}
	[ns]		$/10^7$ s^{-1}	$/10^7$ s^{-1}	[ns]		$/10^7$ s^{-1}	$/10^7$ s^{-1}
THF	0.975	0.506	51.90	50.67	1.742	0.33	18.94	38.46
DCM	0.640	0.359	56.09	100.16	1.600	0.39	24.38	38.13
DMSO	0.813	0.234	28.78	94.22	1.30	0.25	19.23	57.69
ACN	0.274	0.036	13.18	351.79	0.944	0.18	19.07	86.86
EtOH	0.649	0.267	41.14	112.94	1.140	0.33	28.95	58.77
MeOH	0.277	0.150	54.15	306.86	1.750	0.21	12	45.14

Every modification that reduces the rotational ability of indolenine groups can increase quantum yield, lifetimes and thus may provide an enhancement of the performance of resulting solar cells. When this rotation is inhibited, e.g. due to the presence of long alkyl chains, the quantum yield increases.

Fluorescence decay acquired by lifetime measurements in all the solvents was fitted by a mono-exponential function and only in a few cases a bi-exponential function was used. The analysis of the data presented in Table 3-SI shows that, in general, the increase of solvent polarity causes a reduction in the observed lifetime. The introduction of long alkyl chains can increase considerably the lifetime. The lifetime of VG1-C10 was nearly doubled with respect to the reference structure SQ01 already reported.

As a final confirmation, if we take into account some relationships between quantum yield and lifetimes:

$$\varphi_f = \frac{k_f}{k_f + k_{nr}} \quad \text{(eq. 4)}; \qquad \tau = \frac{1}{k_f + k_{nr}} \quad \text{(eq. 5)}; \qquad k_f = \frac{\phi_f}{\tau_f} \quad \text{(eq. 6)}$$

$$k_{nr}^{tot} = k_f(\phi_f^{-1} - 1) \qquad \text{(eq. 7)}$$

We could obtain the constant that account for all the non-radiative processes that reduce fluorescence. Obviously, the non-radiative process that suppresses fluorescence is more efficient in polar solvents. At the same time, the addition of longer alkyl chains into the indolenines causes a consistent reduction of these processes, in agreement with the previously demonstrated increase of lifetimes and quantum yields.

In order to explain and rationalize our results, we refer to a twisted intramolecular charge transfer state (TICT) mechanism, which was first proposed for cyanine and was found to be valid also for squaraines accounting for their very short lifetimes and low quantum yield.[4] This TICT mechanism also accounts for the substantially higher reduction of squaraine lifetimes obtained in polar solvents comparing to the less polar ones.

The addition of two carboxyl and two alkyl chains into a squaraine (from SQ1 to VG1-C10) reduces the rotational ability of indolenine moieties, thus increasing lifetimes and quantum yields.

Taking into account all the above stated reasons VG1-C10 has been chosen as the most perspective squaraine for the fabrication of the hybrid dye-QDs sensitized solar cells.

[4] Tatikolov, A.S.; Costa, S.N.B. *J. Photochem. Photobiol.. (2001), 140, 147-156; b)* Gude C.; Rettig, W. *J. Phys. Chem. A* (2000),104, 8050-8057; c) Rettig, W. In *Electron Transfer I; Mattay, J., Ed.; Topics in Current Chemistry*, Vol. 169; Springer-Verlag: Berlin, 1994

4. Fabrication and characterization of the solar cells

TiO_2 double layer film composed of 8 μm transparent and 5 μm scattering layers was prepared by screen-printing and treated with a 40mM titanium tetrachloride solution as previously reported[2]. The films were heated at 500 °C in air for 30 min before use, then dipped in 0.5 mM dye solutions in ethanol containing 10 mM 3α,7α-dihydroxy-5β-cholic acid (chenodeoxycholic acid, CDCA) for overnight at room temperature. Before the QDs deposition the electrodes were rinsed with ethanol. The CdSe QDs were spin coated on top of the dye-covered titania layer at 2500 rpm for 10 s from a solution with a concentration of approx. 50mg/ml. After the QDs deposition, the solar cells fabrication was completed according to the procedure previously reported[2].The cobalt electrolyte consisted of 0.22M [Co(II)- $(bpy)_3](B(CN)_4)_2$, 0.05 M $[Co(III)(bpy)_3](B(CN)_4)_3$, 0.1 M $LiClO_4$, and 0.2 M tert-butylpyridine in acetonitrile[3].

Photovoltaic measurements have been performed as described in reference [4]. An AM 1.5 solar simulator equipped with a 450W xenon lamp (Model No. 81172, Oriel) with output calibrated to 100 MW cm^2 using a reference Si photodiode containing an IR-cutoff filter (KG-3, Schott) in order to reduce the mismatch between the simulated light and AM 1.5 (in the region of 350–750 nm) to less than 2% with measurements verified at two PV calibration laboratories [ISE (Germany), NREL (USA)]. I–V curves were obtained by applying an external bias to the cell and measuring the generated photocurrent with a Keithley model 2400 digital source meter. The voltage step and delay time of the photocurrent were 10 mV and 40 ms, respectively. The photovoltaic measurements were taken using a metal mask with an aperture area of 0.159 cm^2. A similar data acquisition system was used to determine the monochromatic incident photon-to-electric current conversion efficiency. Under full computer control, light from a 300 W xenon lamp (ILC Technology, USA) was focused through a Gemini-180 double monochromator (Jobin Yvon Ltd., U.K.) onto the photovoltaic cell under test. The monochromator was incremented through the visible spectrum to generate the IPCE (λ) as defined by IPCE (λ) 1⁄4 12400(Jsc/λφ), where λ is the wavelength, Jsc is the short-circuit photocurrent density (mA cm^{-2}), and φ is the incident radiative flux (mW cm^{-2}).

[1] M. Grabolle, M. Spieles, V. Lesnyak, N. Gaponik, A. Eychmüller, U. Resch-Genger, *Anal. Chem.*, **2009**, 81, 6285-6294.

[2] M. K. Nazeeruddin, F. De Angelis, S. Fantacci, A. Selloni, G. Viscardi, P. Liska, S. Ito, B.Takeru, M. Grätzel, *J. Am. Chem. Soc*. **2005**, 127, 16835;

[3] H. N. Tsao, C. Yi, T. Moehl, J.-H. Yum, S. M. Zakeeruddin, M. K. Nazeeruddin, and M. Grätzel, *ChemSusChem*, **2011**, 4, 591 – 594.

[4] J. S. Bendall, L. Etgar, S. C. Tan, N. Cai, P. Wang, S. M. Zakeeruddin, M. Grätzel, M. E. Welland, *Energy Environ. Sci*., **2011**, DOI: 10.1039/c1ee01254a.